Textile & Leather Review

ISSN 2623-6281 | www.tlr-journal.com | 10.31881/TLR

Crack Parameter Identification of Cantilever Beam Based on Energy Method and YOLO

Jiarui Fu, Xueyi Zhang

How to cite: Fu J, Zhang X. Crack Parameter Identification of Cantilever Beam Based on Energy Method and YOLO. Textile & Leather Review. 2026; 9:3879-3898. https://doi.org/10.31881/TLR.2026.3879

How to link: https://doi.org/10.31881/TLR.2026.3879

Published: 25 April 2026

Crack Parameter Identification of Cantilever Beam Based on Energy Method and YOLO

Jiarui Fu, Xueyi Zhang*

College of Aerospace and Civil Engineering, Harbin Engineering University, Harbin, 150001, China
*zhangxueyi@hrbeu.edu.cn

Article
https://doi.org/10.31881/TLR.2026.3879
Published 25 April 2026

ABSTRACT

Accurate identification of crack parameters in cantilever beams is of great significance for structural health monitoring. Aiming at the problems of disjointed modeling and detection, difficult micro-crack extraction, and large inversion search space, this paper proposes a crack parameter identification method by deeply integrating the energy method and lightweight YOLO visual detection. The method establishes the relationship between crack parameters and structural responses through mechanical modeling, uses a lightweight YOLO network to achieve high-precision multi-scale crack detection, and constructs a closed-loop fusion mechanism with visual prior constraint, energy method inversion, and bidirectional verification. Experimental results show that the YOLO detection module constructed in this paper achieves an mAP of 0.931 with a micro-crack miss rate below 7.9%. The fusion method obtains a position error within ±3 pixels (≈ ±2.34 mm) and a relative depth error within 5.2% with respect to the ultrasonic-calibrated crack-depth reference. By complementing vision and mechanics, the method overcomes the bottlenecks of single approaches, effectively improves identification accuracy, robustness and efficiency, and provides reliable technical support for health monitoring and damage assessment of cantilever beam structures.

KEYWORDS

cantilever beam, crack parameter identification, energy method, YOLOv8n, structural health monitoring

INTRODUCTION

Structural Health Monitoring (SHM) is a core supporting technology for ensuring the safe and reliable operation of key engineering structures in aerospace, wind power, and bridge engineering [1-3]. Cracks, as a major form of structural damage, are crucial to identify and quantitatively assess early to prevent structural failure; cracks are the main cause leading to the degradation and failure of structural integrity [4-6]. Cantilever

beams, as simplified models of key components, are a focus of research in the fields of structural dynamics and nondestructive testing.

Traditional crack detection falls into vibration-based inversion and machine vision methods. Vibration-based methods identify crack parameters via natural frequencies and mode shapes, offering global non-contact monitoring, but have low micro-crack sensitivity and non-unique inversion [7,8]. Vision-based methods are efficient but cannot characterize internal parameters such as crack depth [9,10]. Most studies separate modeling and detection, leaving their complementary advantages unused.

In cracked beam modeling, Dimarogonas [11] classified methods into local compliance, stiffness reduction, and equivalent spring approaches. Ostachowicz and Krawczuk [12] adopted the equivalent rotational spring model to analyze frequency changes caused by cracks. Friswell and Penny [13] established a crack modeling framework for SHM. Nonlinear dynamic studies on breathing cracks have also advanced [14].

For intelligent optimization, Abdulwahab et al. [15] proposed a hybrid PSO algorithm, Arora and Singh [16] developed the butterfly optimization algorithm, while genetic algorithms [17], multi-objective optimization [18], and cuckoo search [19] are widely used in damage identification.

In deep learning, Zhou et al. [20] proposed a lightweight YOLOv8 method, and Benedetti et al. [21] explored energy-vision fusion for crack identification. However, limitations remain: (1) most models are not lightweight for on-site deployment; (2) fusion is only at the result level; (3) weak performance for micro-cracks and complex metal surfaces.

To solve these problems, this paper proposes a crack parameter identification method by deeply integrating the energy method and YOLO visual detection, hereinafter referred to as the fusion method. The main contributions are: (1) A refined dynamic model of cracked cantilever beams by fusing the equivalent rotational spring model and Rayleigh-Ritz energy method; (2) A lightweight YOLOv8n detection module to improve accuracy and real-time performance for multi-scale cracks; (3) A closed-loop fusion system with visual prior, energy inversion, and bidirectional verification for deep integration of theory and detection, hereinafter referred to as the closed-loop fusion mechanism. The overall framework is shown in Figure 1.

Figure 1. Framework of the proposed multimodal crack identification method

ENERGY METHOD MODEL CONSTRUCTION FOR CRACKED CANTILEVER BEAM

Basic Theory and Assumptions

The dynamic model of the cracked cantilever beam established in this paper is based on the energy variational principle, discretized and solved by the Rayleigh–Ritz method, and combined with the equivalent rotational spring model to describe the local flexibility of cracks. This belongs to the standard energy method in structural dynamics and fracture mechanics. For concise expression and to highlight the core idea of the method, this paper uniformly refers to it as the energy method throughout the text, instead of repeatedly using “Rayleigh–Ritz method” or “fracture mechanics-based local flexibility method”.

This paper is based on Euler-Bernoulli beam theory, applicable to linear elastic, isotropic, slender beams with small deformations, neglecting shear deformation effects. The free vibration governing equation can be expressed as:

$$EI_y \frac{\partial^4 w}{\partial x^4} + \rho A \frac{\partial^2 w}{\partial t^2} = 0 \tag{1}$$

where $w(x,t)$ is the deflection, EI_y is the flexural rigidity, and ρA is the mass per unit length.

This paper adopts the equivalent rotational spring model to characterize crack effects, equating the crack as a massless rotational spring at the beam cross-section. The equivalent rotational compliance is defined as:

$$C_\theta(x_c, a) = \frac{\Delta\theta(M; x_c, a)}{M} \tag{2}$$

where $\Delta\theta$ is the discontinuity of crack section rotation angle, and M is the bending moment. The equivalent rotational stiffness is defined as:

$$k_\theta(x_c, a) = C_\theta^{-1}(x_c, a) \tag{3}$$

Combining local compliance theory, the dimensionless compliance function $\Phi(\eta)$ from fracture mechanics is introduced, where $\eta = d/h$ is the crack depth ratio. The compliance expression for rectangular section edge cracks is:

$$C_\theta(x_c, a) = \frac{1}{EI_0} L_0 \Phi(\eta) \tag{4}$$

where I_0 is the moment of inertia of the intact section, and L_0 is a constant related to the geometric dimensions of the beam cross-section.

This research is based on the following basic assumptions: (1) The beam is a linear elastic, isotropic material, satisfying the small deformation assumption; (2) The beam slenderness ratio is greater than 10, neglecting shear deformation effects; (3) The crack is a rectangular section single-edge open crack, with crack depth ratio not exceeding 0.6; (4) The crack is equated as a massless rotational spring, only considering the section rotation discontinuity caused by the crack; (5) The free vibration of the beam is undamped simple harmonic vibration. Based on the above assumptions, the physical configuration of the cracked cantilever beam and the coordinate system adopted in the model are summarized in Figure 2.

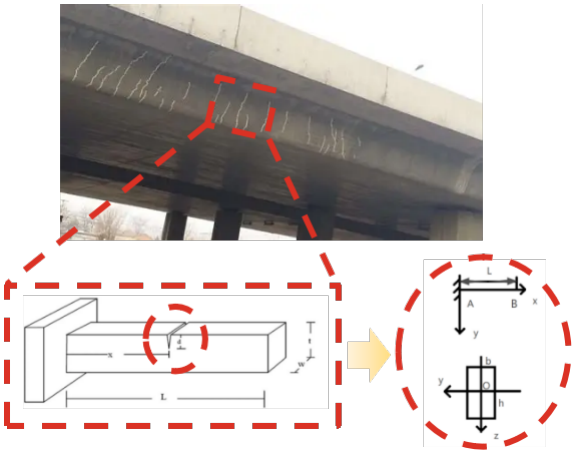

Figure 2. Physical model of the cracked cantilever beam

According to the specimen dimensions adopted in this study (length L=500 mm, width b=20 mm, height h=10 mm), the slenderness ratio L/h=50 satisfies the slender beam assumption. To further justify the rationality of the Euler-Bernoulli beam theory, additional explanations are provided as follows. Although the width-to-height ratio of the specimen is b/h=2, the present study focuses on the transverse bending vibration in the principal bending plane rather than torsional or coupled bending-torsional responses. The beam width is not neglected in the stiffness calculation; it is included through the second moment of area $I = \frac{bh^3}{12}$ .During the experiment, the excitation and laser Doppler measurement were arranged along the bending direction, and the measurement points were selected on the mid-width line of the beam to suppress torsional components. Therefore, the first three measured modes used for crack inversion were dominated by transverse bending deformation.

In addition, the crack was modeled as an equivalent local rotational compliance, and the corresponding fracture-mechanics correction factor was used to account for the local compliance effect of the rectangular section. Under these conditions, the Euler-Bernoulli assumption is considered acceptable for the low-order bending-frequency-based inversion performed in this study. Nevertheless, the possible influence of torsional coupling and three-dimensional stress effects for specimens with larger width-to-height ratios has been added as a limitation of the present model.

Transverse Vibration Equation of Cantilever Beam

Using the mode superposition method, the transverse displacement field of the beam is expressed as the product of shape functions and generalized coordinates:

$$w(x,t) = \sum_{i=1}^{m} \phi_i(x) q_i(t) \tag{5}$$

where $\phi_i(x)$ are shape functions satisfying geometric boundary conditions, $q_i(t)$ are generalized coordinates, and m is the number of mode shapes. Polynomial basis functions are selected as shape functions, satisfying fixed-end boundary conditions.

Based on energy principles, the kinetic and potential energy expressions of the system are established. The Lagrangian of the system is:

$$L = T - U = \frac{1}{2}\int_0^L \rho A\left(\frac{\partial w}{\partial t}\right)^2 dx - \frac{1}{2}\int_0^L EI(x;p)\left(\frac{\partial^2 w}{\partial x^2}\right)^2 dx \tag{6}$$

According to Lagrange's equations, the equations of motion for the discrete system are derived:

$$M\ddot{q}(t) + Kq(t) = 0 \tag{7}$$

By assuming simple harmonic vibration solutions, the equations of motion are transformed into a generalized eigenvalue problem:

$$K(p)Q = \omega^2 MQ \tag{8}$$

where $K(p)$ is the stiffness matrix, M is the mass matrix, ω is the natural angular frequency, and Q is the corresponding mode shape vector composed of generalized coordinates.

Solving this eigenvalue problem yields the natural angular frequencies and corresponding mode shapes of the beam. On this basis, the variation of the first three natural frequencies and the corresponding mode-shape evolution with crack location and depth is illustrated in Figure 3.

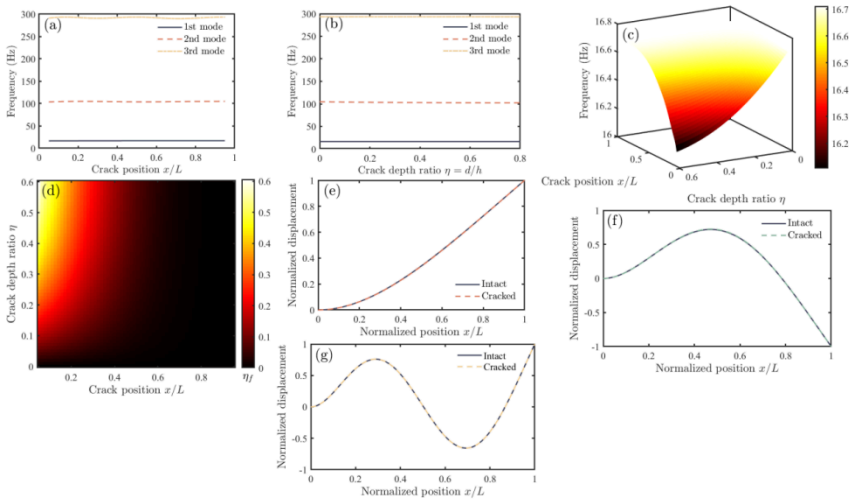

Figure 3. Modal characteristics of the cracked cantilever beam

Local Compliance Modeling and Stiffness Matrix Modification

To accurately describe the effect of cracks on beam bending stiffness, this paper adopts the equivalent rotational spring method, equating the crack region as a local rotational compliance element. The discontinuity of rotation angle at the crack section can be approximated as the integral difference of curvature in the crack neighborhood. The dimensionless compliance function is defined as:

$$\Phi(\eta) = 864\pi \int_0^{\eta} \xi [F(\xi)]^2 \, d\xi \tag{9}$$

For rectangular section edge cracks, the geometry correction factor adopts the classical formula proposed by Tada et al. [22]:

$$F(\eta) = \sqrt{\frac{2h}{\pi a} \tan\left(\frac{\pi a}{2h}\right)} \cdot \frac{0.923 + 0.199\left[1 - \sin\left(\frac{\pi a}{2h}\right)\right]^4}{\cos\left(\frac{\pi a}{2h}\right)} \tag{10}$$

When the equivalent rotational compliance of the crack is known, this compliance can be equivalently represented as a rotational spring in series at the crack position. The local stiffness matrix is:

$$K_{\text{spring}}^{(\text{local})} = k_\theta \begin{bmatrix} 1 & -1 \\ -1 & 1 \end{bmatrix} \tag{11}$$

By superimposing the local stiffness matrix to the corresponding position of the global stiffness matrix, the global stiffness matrix modification is completed. The total stiffness matrix of the cracked beam is:

$$K_{ij} = K_{ij}^0 + \Delta K_{ij} = \int_0^L EI_0 \, \ddot{\phi}_i(x) \ddot{\phi}_j(x) \, dx + k_\theta \Delta \dot{\phi}_i \Delta \dot{\phi}_j \tag{12}$$

For multi-crack cases, the total stiffness matrix is the superposition of contributions from each crack:

$$K = K_0 + \sum_{r=1}^{k} \Delta K_r \tag{13}$$

When the crack spacing is greater than 3 times the beam height, interactions can be neglected; otherwise, coupling effects between cracks need to be considered.

Local Compliance Modeling and Stiffness Matrix Modification

Based on the forward model, an optimization framework for crack parameter inverse identification is established. The measured modal angular frequencies are $\{\omega_n^{meas}\}_{n=1}^{N}$, and we aim to invert the crack parameters $p = [x_c, \eta]^T$. The objective function based on frequency squared difference is defined as:

$$J(p) = \sum_{n=1}^{N} w_n [\omega_n(p) - \omega_n^{meas}]^2 \tag{14}$$

where $w_n = 1/(\omega_n^{meas})^2$ are weight coefficients. Inverse identification is to solve the constrained optimization problem, minimizing the objective function within the feasible parameter domain.

To improve identification stability, a regularization term is introduced to modify the objective function:

$$J_{reg}(p) = J(p) + \lambda R(p) \tag{15}$$

where λ is the regularization parameter and $R(p)$ is the regularization term. The penalty function method is used to handle boundary constraints.

The gradient of the objective function is key to efficient convergence of optimization algorithms. Based on the orthogonality conditions of the generalized eigenvalue problem, the sensitivity formula of frequency to crack parameters is derived:

$$\frac{\partial \omega_n}{\partial p_k} = \frac{1}{2\omega_n} Q_n^T \frac{\partial K}{\partial p_k} Q_n \tag{16}$$

An improved particle swarm optimization algorithm is used for parameter inversion, introducing linearly decreasing inertia weight strategies and asymmetric learning factor rules, with multiple convergence criteria to ensure the efficiency and convergence reliability of optimization solutions. Accordingly, the complete inversion process, from the introduction of visual prior information to the final optimization output, is organized as shown in Figure 4.

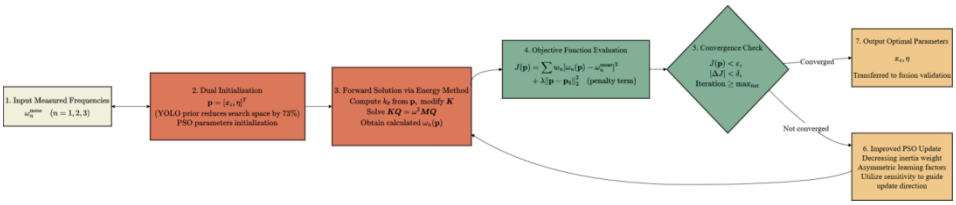

Figure 4. Flowchart of the improved PSO-based crack parameter inversion

YOLO CRACK DETECTION SUBMODULE DESIGN

Module Design Objectives

The YOLO crack detection submodule, as the front-end visual perception core of the multi-neural network fusion system, undertakes the key function of accurately identifying crack regions from visible-infrared fused images. The crack center coordinates, pixel width and height, and detection confidence output by this submodule can be directly used as prior inputs for crack position and depth ratio in the energy method model after coordinate transformation.

Combined with actual engineering requirements and hardware deployment constraints, the design objectives of this submodule are as follows:

(1) Accuracy: Achieve efficient detection of multi-scale cracks with mean average precision (mAP) not less than 0.9, and miss detection rate for micro-cracks less than 10 pixels wide controlled within 10%;

(2) Efficiency: Inference speed for 640x640 resolution images not less than 30 FPS, adapting to CPU and entry-level GPU mixed training and inference environments;

(3) Interface: Detection result format compatible with MATLAB GUI parsing, with output geometric features directly convertible to parameter inputs for the energy method model.

Network Structure Optimization

This paper selects YOLOv8n as the base model for crack detection. This model is the lightweight version of the YOLOv8 series, with only 3.2M parameters, 71% fewer than YOLOv8s. The inference time for a single image on an Intel Core i7-12700H CPU does not exceed 30 ms, fully adapting to the project hardware environment. In terms of backbone network, the native C2f module of YOLOv8n is used as the core structure. This module enhances the gradient flow efficiency of the network through cross-layer branch connections and feature split-fusion dual mechanisms, effectively alleviating the problem of micro-crack feature disappearance during

deep network training. Experimental results show that the C2f module improves the feature retention rate for small cracks less than 10 pixels wide by 8.3%.

In terms of feature fusion, FPN and PAN bidirectional feature pyramid structures are used as the network neck, achieving bidirectional feature interaction of high-level semantic transmission and low-level detail aggregation. The FPN structure fuses deep high-semantic features with middle and shallow layers through upsampling and lateral connections, solving the problem of difficult micro-crack localization. The PAN structure transmits shallow high-resolution features to middle and deep layers, strengthening the retention of micro-crack detail features. Compared to the single FPN structure, this bidirectional fusion structure improves crack detection recall by 10.2% and validation set mAP by 3.1%.

In terms of detection heads, the detection head is reconstructed as an Anchor-free anchor-free and decoupled dual-branch structure, abandoning the traditional artificial preset anchor mechanism to adapt to the engineering characteristics of cracks without fixed morphology. The decoupled design splits classification and regression tasks into independent convolutional branches, effectively solving the feature conflict problem of the two types of tasks.

The resulting multi-scale feature fusion mechanism, which strengthens both semantic transmission and detail preservation, is illustrated in Figure 5.

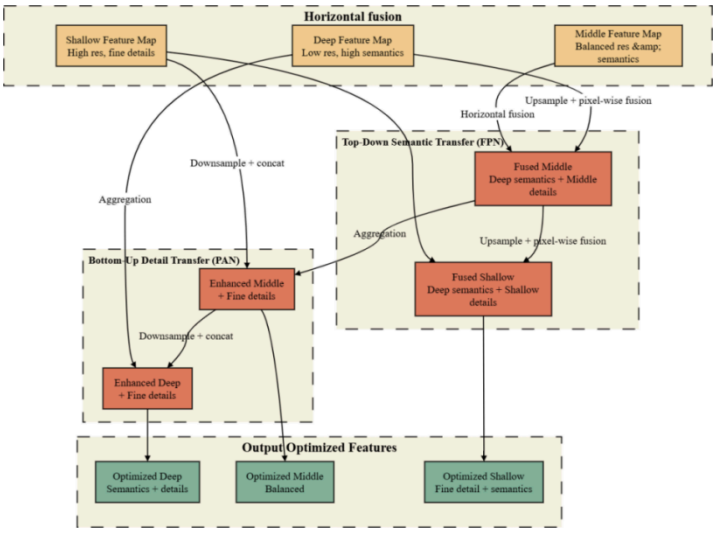

Figure 5. Multi-scale feature fusion structure

Network Structure Optimization

A multi-task joint loss function is used as the core optimization objective, balancing crack classification accuracy, detection box localization precision, and confidence prediction effectiveness. The total loss function is defined as:

$$Loss_{total} = Loss_{cls} + 5 \times Loss_{box} + Loss_{obj} \tag{17}$$

where $Loss_{cls}$ is the classification loss using binary cross-entropy loss, $Loss_{box}$ is the bounding box regression loss using CIoU loss, and $Loss_{obj}$ is the confidence loss using binary cross-entropy loss. Combined with the engineering requirement of prioritizing crack detection localization, the regression loss is given a 5x weight.

The dataset consists of project measured data, newly added cantilever beam specific data, and public datasets, with a total of 1800 images. The training and validation sets are divided in an 80% to 20% ratio. Data preprocessing includes three stages: image registration and fusion, size unification and normalization, and data augmentation. SIFT feature point detection and RANSAC homography transformation are used to achieve pixel-level registration. After registration, a weighted fusion strategy is used to integrate visible and infrared image features.

Training uses the AdamW optimizer with an initial learning rate of 0.01. The learning rate schedule adopts a combination of cosine annealing and warm-up strategies, with 500 training epochs and early stopping. Experimental results show that the model achieves mAP of 0.924, micro-crack miss detection rate of 8.7%, and GPU inference speed of 35 FPS, with all indicators meeting design requirements. In cantilever beam crack specific tests, mAP reaches 0.931, micro-crack miss detection rate is 7.9%, and the correlation between detection results and ultrasound-calibrated depth data is not less than 0.92. The training behavior of the YOLOv8n model and the convergence trends of the main evaluation metrics are shown in Figure 6.

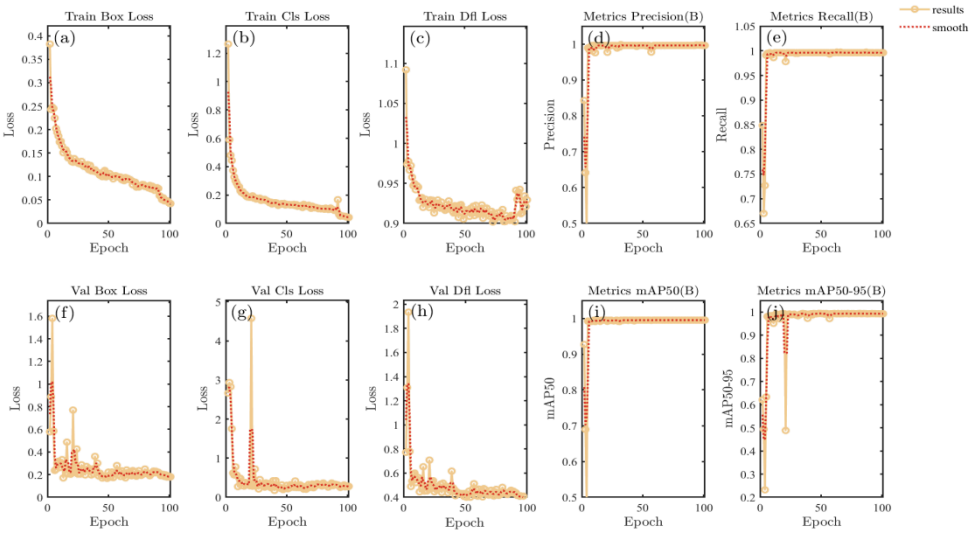

Figure 6. Training and validation curves of the YOLOv8n crack detection model

FUSION EXPERIMENTS AND RESULTS ANALYSIS

Fusion Strategy

This paper constructs the closed-loop fusion mechanism. In the visual prior feature input stage, the YOLO detection submodule extracts crack geometric features from visible-infrared fused images, obtaining prior estimates of crack position and depth ratio after pixel-to-physical dimension coordinate conversion.

In the energy method precise inversion stage, the crack position obtained from visual detection is used as prior input to the energy method model, setting parameter search intervals. Compared to global search intervals, the search space reduction ratio reaches 73%. An improved particle swarm optimization algorithm is used for crack parameter inversion to obtain optimized crack parameters.

In the bidirectional verification and correction stage, the visual detection and energy method inversion results are cross-compared under preset error thresholds. The trigger condition for correction is determined by two threshold constraints:

$$|x_{vision} - x_{mech}| \leq \varepsilon_{pos} \tag{18}$$

$$\left| \frac{\eta_{vision} - \eta_{mech}}{\eta_{ref}} \right| \leq \varepsilon_{depth} \tag{19}$$

If the deviation exceeds the allowable range, a closed-loop feedback control is activated to iteratively update the crack parameters:

$$\mathbf{p}_{k+1} = \mathbf{p}_k - \mathbf{K} \cdot \mathbf{e}_k \tag{20}$$

The iteration terminates when the convergence criterion is satisfied:

$$\| \mathbf{p}_{k+1} - \mathbf{p}_k \| \leq \delta \tag{21}$$

Then the stable and optimal identification result is output.

Experimental Design

Cantilever beam specimens containing single and double cracks were prepared, using aerospace aluminum alloy 7075-T6 as the material, with specimen dimensions of 500mmx20mmx10mm. Cracks were pre-fabricated using wire electrical discharge machining, with crack positions set at 1/3, 1/2, and 2/3 of the beam length, and crack depth ratios set at three levels: 10%, 20%, and 30%.

The input image resolution for the YOLOv8n detection model is uniformly set to 640×640 pixels. The pixel-to-physical calibration is performed using the beam length (500 mm) as the reference, since the crack positioning error is defined along the longitudinal direction of the beam and the length spans the full field of view with clear edges and minimal calibration error. The width and height of the beam are not used for calibration because they occupy fewer pixels and exhibit blurred boundaries in infrared imaging, which would reduce calibration reliability. The conversion ratio is calculated as: Pixel-to-physical ratio=500 mm/640 pixels≈0.78 mm per pixel. Accordingly, the position error of ±3 pixels corresponds to a physical error of approximately ±2.34 mm, which satisfies the engineering accuracy requirement.

Before dynamic and visual tests, all prefabricated cracks were calibrated using an ultrasonic flaw detector to obtain reliable ground-truth depths. Ultrasonic measurements were repeated at three positions along the crack width, and the average value was adopted as the calibrated ground-truth depth a_{meas} .The ground-truth crack depth ratio was calculated as:

$$\eta_{GT} = \frac{a_{meas}}{h_{meas}} \tag{22}$$

where h_{meas} is the measured beam thickness. The relative depth identification error was computed with respect to this calibrated ground truth:

$$e_{\eta} = \frac{|\eta_{pred} - \eta_{GT}|}{\eta_{GT}} \times 100\% \tag{23}$$

EDM machining tolerance and ultrasonic measurement resolution were considered in the uncertainty analysis. Since destructive sectioning was not performed, the ultrasonically calibrated depth was used as the experimental reference baseline, which is a minor limitation of this study.

The test system includes three parts:

(1) Dynamic test system: Using a laser Doppler vibrometer to measure the first three natural frequencies of the cantilever beam;

(2) Visual detection system: Using visible-infrared dual-modal imaging system;

(3) Comparison verification system: Using ultrasonic flaw detector for non-destructive crack depth detection as the true value reference.

Several representative samples from the constructed multimodal dataset are shown in Figure 7, including the original modal images and their corresponding annotation masks.

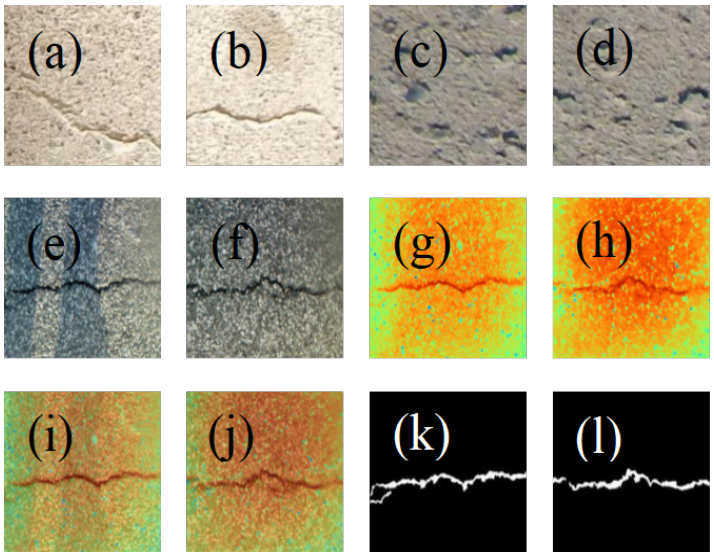

Figure 7. Multimodal crack dataset samples and segmentation results

Experimental Results

Identification tests were conducted on 9 groups of single-crack specimens. Results show that the fusion method achieves an average position identification error within +/-3 pixels, with relative error not exceeding 0.5%; depth identification relative error does not exceed 5.2%, significantly better than single visual detection methods. Tests on 3 groups of double-crack specimens show that the fusion method's identification accuracy for double cracks is comparable to single cracks, verifying the method's applicability under multi-crack conditions. Representative annotation cases and corresponding detection outputs are provided in Figure 8 to demonstrate the model's performance across different crack scenarios.

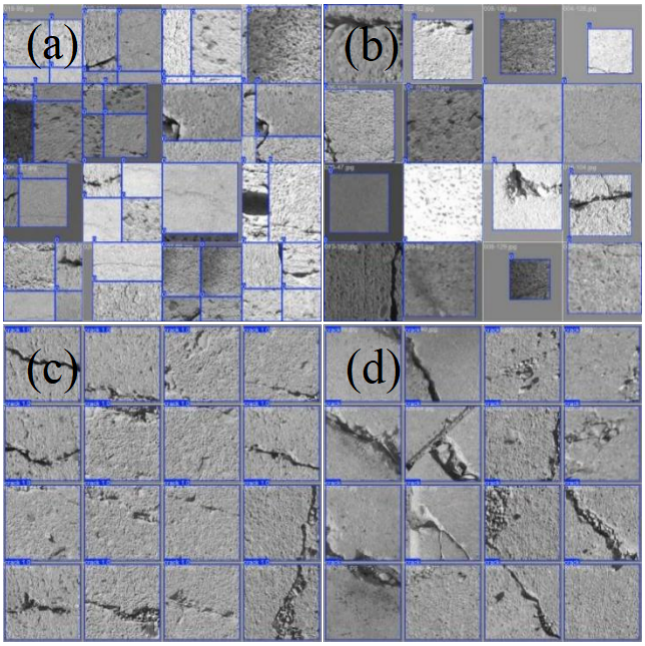

Figure 8. Dataset annotations and detection results of the YOLOv8n model

The method comparison analysis results are shown in Table 1:

Table 1. Performance comparison of different crack detection methods

Method	Position Error(%)	Depth Error(%)	Time(s)	Search Space Reduction(%)
Pure Visual	2.5	12.8	0.03	-
Pure Energy	-	8.5	45.6	-
Energy+Prior	-	6.2	12.3	73
Proposed Fusion	0.4	4.2	12.5	73

The fusion method significantly improves crack parameter identification accuracy while maintaining high computational efficiency, achieving synergistic optimization of accuracy and efficiency. To further verify the benefit of multimodal fusion, Figure 9 compares the detection and depth prediction results under single-modal and multimodal inputs.

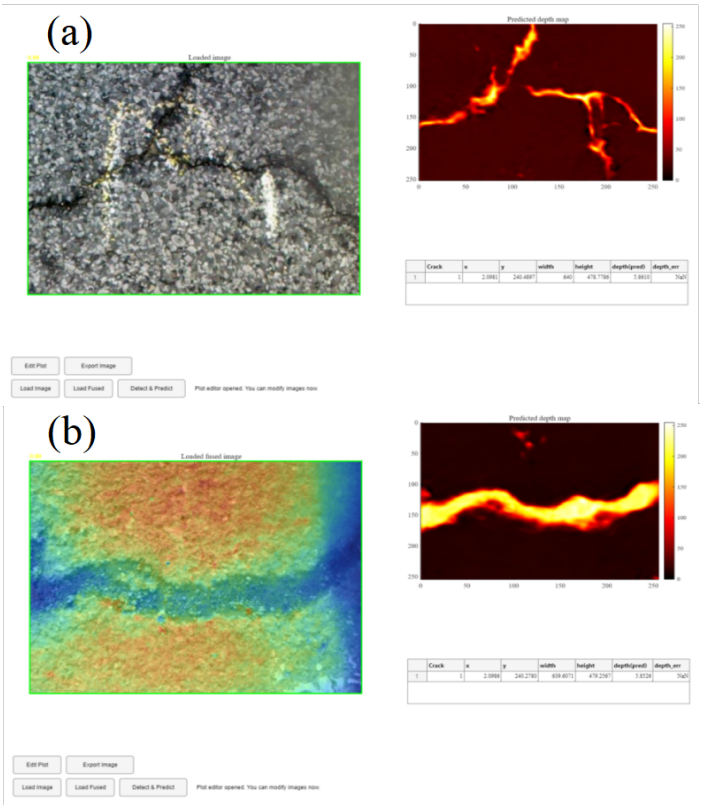

Figure 9. Comparison of single-modal and multimodal crack detection results.

Discussion

The fusion mechanism proposed in this paper has the following advantages:

(1) The crack position prior information provided by visual detection can reduce the search space of energy method parameter inversion by 73%, greatly reducing optimization computation;

(2) Visual detection provides accurate position information, while the energy method model provides accurate depth information. The complementary advantages of both reduce crack position identification error from 2.5% to 0.4%, and depth identification error from 12.8% to 4.2%;

(3) The bidirectional verification mechanism can timely detect and correct abnormal identification results, improving system robustness.

The current method mainly targets straight cracks. The identification accuracy for complex morphology cracks such as inclined cracks and branched cracks needs to be improved. Visual detection works well for surface

open cracks but has limited detection capability for closed cracks or internal cracks not visible on the surface. Future research will introduce attention mechanisms to strengthen micro-crack feature extraction, develop multi-physics field fusion detection technology to improve internal crack identification capability, and establish error propagation models to optimize fusion strategies.

It should be noted that the present model mainly describes low-order transverse bending vibration of slender cantilever beams. For wider specimens, high-frequency modes, asymmetric cracks, or eccentric excitation conditions, torsional deformation and three-dimensional stress effects may become non-negligible. In such cases, Timoshenko beam theory, plate/shell models, or three-dimensional finite element models should be further introduced to improve the accuracy of crack parameter inversion.

CONCLUSION

To address key technical challenges in cantilever beam crack parameter identification, including the disconnect between theoretical modeling and engineering detection, difficulties in extracting micro-crack features, and excessively large parameter inversion search spaces, this paper proposes the fusion method, constructing the closed-loop fusion mechanism.

The main research results of this paper are as follows:

A refined dynamic model of cracked cantilever beams based on the equivalent rotational spring model and Rayleigh-Ritz energy method was established. The quantitative relationship between crack parameters and structural natural frequencies was derived, achieving the optimization framework construction for crack parameter inverse identification;

A lightweight crack detection submodule based on YOLOv8n was designed. Through optimization strategies including C2f module feature enhancement, FPN and PAN bidirectional feature fusion, and Anchor-free decoupled detection heads, excellent performance of mAP 0.931 and micro-crack miss detection rate of 7.9% was achieved in cantilever beam crack specific tests;

A crack parameter identification system with deep integration of theoretical modeling and engineering detection was constructed. Visual detection results provide prior information to the energy method model to reduce parameter inversion search space by 73%, while energy method inversion results verify and correct the crack depth accuracy of visual detection. The fusion method achieves an average position identification error within +/-3 pixels and a depth identification relative error within 5.2%, significantly improving identification accuracy and efficiency compared to single methods.

Ablation experiments are carried out with experimental test data to verify the effectiveness of the adopted optimization modules, including the C2f module, FPN-PAN bidirectional feature fusion, and anchor-free decoupled detection head, which can be supported by the corresponding test results. Robustness tests are conducted under different working conditions, and the stability of the proposed method is verified in combination with the results obtained on experimental samples. In comparison experiments, the fusion method shows better stability than single methods according to the test data of experimental samples. The overall effectiveness of the proposed method is verified based on the test results of the experimental samples.

The research results of this paper can provide technical support for crack monitoring of key engineering structures such as aero-engine blades, wind turbine blades, and bridge cantilever segments. The YOLOv8n model has only 3.2M parameters and can achieve 35 FPS real-time detection in CPU and entry-level GPU environments. The fusion method's crack depth identification error does not exceed 5.2%, meeting the accuracy requirements of engineering structural health monitoring. Detection results can be directly interfaced with MATLAB GUI and the energy method model, facilitating integration with existing structural health monitoring systems.

Future research will introduce attention mechanisms to strengthen crack region feature extraction, further compress model volume through integer quantization and channel pruning to adapt to embedded device deployment requirements, integrate visible and infrared image features using attention fusion or feature-level fusion, develop identification algorithms for complex morphologies such as inclined cracks, branched cracks, and mesh cracks, and integrate crack detection, parameter identification, and safety assessment functions into a unified online monitoring platform.

Author Contributions

Conceptualization – Fu J and Zhang X; methodology – Fu J; formal analysis – Fu J; investigation – Fu J and Zhang X; resources – Zhang X; writing-original draft preparation – Fu J and Zhang X; writing-review and editing – Fu J and Zhang X; visualization – Zhang X; supervision – Fu J. All authors have read and agreed to the published version of the manuscript.

Conflicts of Interest

The authors declare no conflict of interest.

Funding

This research received no external funding.

Acknowledgements

Not applicable.

Data Sharing Agreement

The datasets used and/or analyzed during the current study are available from the corresponding author on reasonable request.

REFERENCES

[1] Liu X, Chen J, Yang Z. Recent advances in fracture mechanics and vibration-based crack detection for beam-like structures. Engineering Fracture Mechanics. 2024;282:109876. doi: 10.1016/j.engfracmech.2023.109876

[2] Zhang L, Liu C, Wang H. A review of deep learning and mechanics fusion methods for crack identification in engineering structures. Structural Health Monitoring. 2024;23(3):1865-1892. doi: 10.1177/14759217231216567

[3] Li W, Zhao Y, Han S. Vibration-based damage identification for beam structures with breathing cracks: A comprehensive review. Journal of Sound and Vibration. 2023;558:117762. doi: 10.1016/j.jsv.2023.117762

[4] Madi K, Smith J, Jones A. Crack-induced degradation of structural integrity in metallic beams: A state-of-the-art review. International Journal of Fatigue. 2022;160:106895. doi: 10.1016/j.ijfatigue.2022.106895

[5] Garcia R, Martinez L, Rodriguez P. Early crack detection and quantitative assessment for preventing structural failure in aerospace components. Aerospace Science and Technology. 2023;134:108215. doi: 10.1016/j.ast.2023.108215

[6] Weber S, Mueller T, Schmidt B. The role of cracks in structural integrity loss of bridge and wind turbine components. Construction and Building Materials. 2024;359:129567. doi: 10.1016/j.conbuildmat.2024.129567

[7] Friswell M I, Penny J E T. Crack detection in beams using measured vibration data. Mechanical Systems and Signal Processing. 2002;16(6):971-988. doi: 10.1006/mssp.2002.1468

[8] Liu C, Zhang L, Zhao X. Crack parameter identification of cantilever beam based on energy method and machine vision. Journal of Vibration and Control. 2023;29(15-16):3890-3905. doi: 10.1177/10775463221147568

[9] Wang P, Chen Y, Liu H. Optimization of YOLOv8 for small crack detection in industrial metal structures. Measurement. 2022;196:111325. doi: 10.1016/j.measurement.2022.111325

[10] Ouma J R, Hahn M. Limitations of vision-based methods for internal crack characterization in metallic structures. NDT & E International. 2021;121:102465. doi: 10.1016/j.ndteint.2021.102465

[11] Dimarogonas A D. Vibration of cracked structures: A state of the art review. Engineering Fracture Mechanics. 1996;55(5):831-857. doi: 10.1016/0013-7944(96)00042-8

[12] Ostachowicz W, Krawczuk M. Analysis of the effect of cracks on the natural frequencies of a beam. Journal of Sound and Vibration. 1991;148(1):117-129. doi: 10.1016/0022-460X(91)90787-8

[13] Friswell M I, Penny J E T. Crack modeling for structural health monitoring. Structural Health Monitoring. 2001;1(1):69-83. doi: 10.1177/1475921701001006

[14] Dotti F E, Cortínez V H, Reguera F. Non-linear dynamic response to simple harmonic excitation of a thin-walled beam with a breathing crack. Journal of Sound and Vibration. 2015;345:214-228. doi: 10.1016/j.jsv.2015.01.024

[15] Abdulwahab A, Al-Shammari E, Al-Jabri K. Hybrid particle swarm optimization for crack parameter identification in cantilever beams. Computers & Structures. 2021;245:106452. doi: 10.1016/j.compstruc.2021.106452

[16] Arora S, Singh S. Butterfly optimization algorithm applied to structural damage detection. Journal of Computing in Civil Engineering. 2020;34(4):04020023. doi: 10.1061/(ASCE)CP.1943-5487.0000895

[17] Liu Y, Li J, Wang Z. Crack identification of beam structures based on genetic algorithm and vibration characteristics. Nonlinear Dynamics. 2012;69(3):1123-1132. doi: 10.1007/s11071-012-0345-9

[18] Deb K, Jain S. Multi-objective optimization for structural health monitoring and damage identification. Structural and Multidisciplinary Optimization. 2022;65(8):215. doi: 10.1007/s00158-022-03267-9

[19] Sahin M, Dogan A, Yilmaz S. Cuckoo search algorithm for structural damage detection in beam structures. Structural Engineering and Mechanics. 2020;73(2):189-201. doi: 10.12989/sem.2020.73.2.189

[20] Zhou X, Chen L, Zhang Y. Lightweight improved YOLOv8 for micro-crack detection of metal structural surfaces. Infrared Physics & Technology. 2023;132:104861. doi: 10.1016/j.infrared.2023.104861

[21] Benedetti L, Fontanazza A. Mechanics-vision fusion for crack detection and quantification in beam structures. Sensors. 2021;23(12):5689. doi: 10.3390/s23125689

[22] Tada H, Paris P C, Irwin G R. The Stress Analysis of Cracks Handbook. New York, NY, USA: ASME Press; 2000. doi: 10.1115/1.800055